Electron transport through antidot superlattices in $Si/Si_{0.7}Ge_{0.3}$ heterostructures

D. Többen and M. Holzmann
Walter Schottky Institut, Technische Universität München, D-85748, Garching, Germany

S. Kühn and H. Lorenz
Sektion Physik der Ludwig-Maximilians-Universität München, Geschwister-Scholl-Platz 1, D-80539 München, Germany

G. Abstreiter
Walter Schottky Institut, Technische Universität München, D-85748, Garching, Germany

J. P. Kotthaus
Sektion Physik der Ludwig-Maximilians-Universität München, Geschwister-Scholl-Platz 1, D-80539 München, Germany

F. Schäffler
Daimler-Benz AG, Forschungsinstitut Ulm, Wilhelm-Runge-Strasse 11, D-89081 Ulm, Germany
(Received 6 June 1994)

Transport properties of electrons in antidot superlattices are studied in Si/Ge heterostructures. Lateral superlattices with periods between 830 and 500 nm were imposed upon high-mobility two-dimensional electron gases in $Si/Si_{0.7}Ge_{0.3}$ heterostructures by means of laser holography and reactive ion etching. Typical features known from $GaAs/Al_xGa_{1-x}As$ samples, such as low-field commensurability oscillations in the longitudinal resistivity ρ_{xx}, additional nonquantized Hall plateaus, and quenching of the Hall effect around $B=0$, are observed. From the position of the commensurability maxima in ρ_{xx} we conclude that the lateral potential is rather smooth.

Electron transport in lateral antidot superlattices, i.e., in periodic arrays of purposely introduced scatterers, has been subject to extensive experimental[1-5] and theoretical research[6] throughout the last few years. Various fabrication techniques, such as electron-beam and holographic lithography combined with dry etching, ion bombardment, or electrostatic induction via a patterned gate, were successfully employed to impose a lateral potential modulation upon a high-mobility two-dimensional electron gas (2DEG). Several pronounced magnetotransport anomalies, such as low-field maxima in the longitudinal resistivity ρ_{xx}, additional, nonquantized Hall plateaus in the same regime, and quenching of the Hall effect around $B=0$ have been observed. Very recently, magnetotransport studies in the fractional quantum-Hall-effect regime of electrons in antidot superlattices were also successfully employed to prove the actual existence of composite fermions.[7]

All of these studies were so far conducted only on III-V semiconductors, especially $GaAs/Al_xGa_{1-x}As$ heterostructures, since the elastic mean free path of the electrons has to be larger than the period of the superlattice in order to be able to obtain the above features. Within the last few years, however, the quality of Si/SiGe heterostructures grown on relaxed SiGe buffer layers has strongly improved and electron mobilities in the range of 170 000 cm^2/V s at low temperatures were accomplished by several groups.[8-10] The 2DEG's confined in such samples possess transport properties much more similar to those of $GaAs/Al_xGa_{1-x}As$ heterostructures than to those of Si metal-oxide semiconductor structures.[11] In this work we report on magnetotransport investigations of antidot arrays in such Si/SiGe heterostructures. To the best of our knowledge, this is the first study on the influence of this kind of artificial superlattices on a 2DEG conducted outside of the III-V system.

The n-type modulation-doped $Si/Si_{0.7}Ge_{0.3}$ heterostructures used for lateral patterning were grown at Daimler-Benz on thick, relaxed SiGe buffer layers with linearly increasing Ge content by molecular-beam epitaxy. Details on the growth and the characterization of the 2DEG's have been published elsewhere.[8,11] The electrons are confined to a strained Si channel about 82 nm beneath the surface, separated from the Sb donors by an 11 nm-thick spacer layer of undoped $Si_{0.7}Ge_{0.3}$. At $T=370$ mK an electron mobility of $\mu=175\,000$ cm^2/V s at a sheet density $n_s=6.9\times10^{11}$ cm^{-2} is observed. The elastic mean free path

$$l_{\mathrm{mpf}}=\frac{\hbar\mu}{e}\left[\frac{4\pi n_s}{g_s g_v}\right]^{1/2} \tag{1}$$

in these samples is thus about 1.7 μm, using an effective mass $m^*=0.19m_0$ and spin and valley degeneracies $g_s=g_v=2$.

The samples were covered with 90-nm photoresist film and an interference grating was exposed twice using laser holography, with a 90° rotation of the sample around its surface normal in between. By choosing appropriate exposure and developing times a lattice of voids was created in the photoresist. This pattern was then transferred into the semiconductor by reactive-ion etching using CF_4. After removal of the photoresist mask, the period of the antidot superlattice and the etch depth were checked by

atomic-force microscopy. Periods $a=830$, 620, and 500 nm were realized. The etch depths were about (72 ± 5) nm, i.e., just into the spacer layer, for the two specimens with the smaller periods and, unintentionally, about (62 ± 5) nm for the 830 nm sample. However, also in the latter case, most of the doping layer was removed in each antidot. The ratio of the geometric antidot diameter d_{GEO} to the period a was found to be 0.56 ± 0.05 for the samples with $a=830$ and 620 nm. For the specimen with the smallest period d_{GEO}/a turned out to be somewhat smaller, about 0.48 ± 0.05. The above variations of both the etch depths and the antidot sizes could arise from the crosshatched pattern of height modulation on the surface, which is typical for Si/SiGe heterostructures grown on relaxed graded SiGe buffer layers.[9,10]

After the micropatterning, Hall bars were defined by wet-chemical etching and Ohmic contacts of Sb and Au were deposited and alloyed. The magnetotransport measurements were performed in a ^{3}He cryostat equipped with a superconducting magnet. Standard lock-in technique with a current of 100 nA at 81 Hz was used.

Figure 1 shows the longitudinal resistivities ρ_{xx} of all three patterned samples as well as that of the unstructured reference sample at $T=370$ mK up to $B=8$ T in the dark. Apart from a drastic rise in the resistivity at zero field increasing with decreasing antidot superlattice period, two distinct peaks in the low-field regime below $B=1$ T are clearly observable for each of the three patterned specimens. These maxima shift slightly to higher magnetic fields with decreasing superlattice period. At higher magnetic fields the resistivity decreases and regular Shubnikov–de Haas (SdH) oscillations commence. This regime is used to evaluate the sheet densities n_s, which are equal to that of the reference sample within a few percent. The positions of the two low-field peaks are $r_c/a=(1.51\pm0.10)$ and (0.47 ± 0.03), respectively, for all three samples, with

$$r_c=\frac{\hbar}{eB}\left[\frac{4\pi n_s}{g_s g_v}\right]^{1/2} \tag{2}$$

being the cyclotron radius at the corresponding magnetic field. While a peak at $r_c/a\approx\frac{1}{2}$ is always expected in a periodic lateral potential, perfectly circular, collision-free trajectories at r_c/a equal to $\frac{3}{2}$ cannot exist in a billiard-type model of reflecting disks. We therefore conclude that the lateral potential is rather smooth and that the observed peaks are commensurability maxima associated with pinned electron orbits around one or four antidots.[6] For the samples with periods $a=620$ and 500 nm we also find a shoulder around $r_c/a\approx0.2$, which is indicated by the arrow in Fig. 2(a).

The effective electron mobilities evaluated as

$$\mu_{\mathrm{eff}}=[n_s e\rho_{xx}(B=0)]^{-1} \tag{3}$$

in the samples with periods $a=830$, 620, and 500 nm—as determined from the SdH carrier density and the ρ_{xx} at $B=0$—are 37 200, 14 300 and 8700 cm^2/V s, respectively. This decrease compared to the value of the unstructured sample is brought about not only by the intentionally added scattering centers, but probably also by defects created by imperfect fabrication. It is important to remember that the mean free path of the electrons moving between the antidots is only affected by such defects. It is nevertheless still larger than the superlattice period since the commensurability maxima are well observable. The actual deterioration of the sample quality is illustrated by the fact that the spin and valley degeneracies, ob-

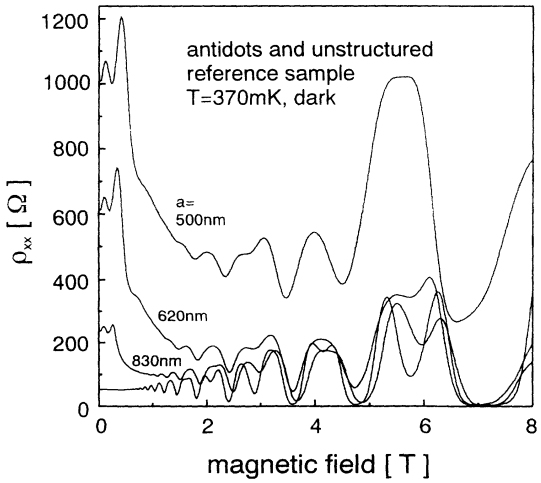

FIG. 1. Longitudinal resistivities ρ_{xx} of antidot samples with periods $a=830$, 620, and 500 nm as well as of an unstructured reference sample at $T=370$ mK up to $B=8$ T in the dark. The carrier density of all specimens is about 7×10^{11} cm^{-2} within a few percent. The ratio r_c/a for the two low-field peaks is (1.51 ± 0.10) and (0.47 ± 0.03), respectively.

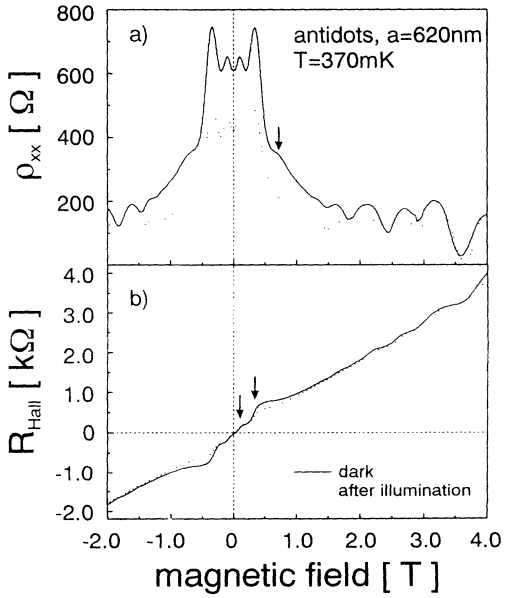

FIG. 2. (a) Longitudinal resistivity ρ_{xx} and (b) Hall resistance R_{Hall} of the sample with period $a=620$ nm in the dark (solid) and after intensive illumination (dashed curves). The arrows indicate the positions (a) of the anomalous shoulder around $r_c/a\approx0.2$, which vanishes with illumination, and (b) of the peaks in ρ_{xx} corresponding to the additional, nonquantized Hall plateaus at low magnetic fields.

served at $B=1.5$ and 4 T in the references sample, are no longer resolved at such relatively low magnetic fields. Also, the longitudinal resistivity of the sample with period $a=500$ nm does not vanish any more even at filling factor $\nu=4$ below $B=7$ T.

By illuminating the samples with a red light-emitting diode, the resistivities can be persistently reduced even though the carrier densities are only negligibly increased as illustrated in Fig. 2(a) for the sample with period $a=620$ nm. Intense illumination of this specimen enhances the effective mobility by almost 50%. Hardly any effect, on the other hand, was seen in the reference sample. The anomalous shoulder mentioned above also vanishes. Since this shoulder is not at all observed in the more shallow etched sample with period $a=830$ nm we believe that it is due to charged defects generated by the—relatively deep—reactive-ion etching. These apparently can be neutralized, at least partially, by illumination resulting in higher electron mobilities. However, it has not yet been possible to find an explanation why the shoulder appears at this particular magnetic field. Further studies involving a passivation step immediately following the etching process should be helpful to better understand the nature of these defects.

Another interesting aspect of Fig. 2(a) is the relative height of the two low-field maxima with respect to each other. While the second peak associated with motion around a single antidot is much higher than the first one in the dark, they are of almost equal amplitude after illumination. This tendency is illustrated in more detail in Fig. 3, which displays the ratio of the peak height ΔR (see inset) and the longitudinal resistance $R=5\rho_{xx}$ at $B=0$ as a function of the effective electron mobility for the sample with period $a=620$ nm. The latter was tuned by short-time illumination. While this relative amplitude remains roughly constant at about 20% for the second peak (filled symbols), the height of the first peak increases with mobility (hollow symbols). The dashed lines are guides to the eye. Obviously the probability for trajectories with four antidots enclosed is enhanced, as expected, as the actual mobility and thereby the elastic mean free path of the electrons is increased by the illumination. Similar behavior was found for the sample with the smallest period $a=500$ nm. The relative peak heights for the sample with the largest period $a=830$ nm are both around 10% in the dark and also after illumination. One should keep in mind, however, that this sample was etched less deeply than the other two. Therefore, one expects the potential modulation to be less pronounced, as well as fewer etch defects reducing the elastic mean free path.

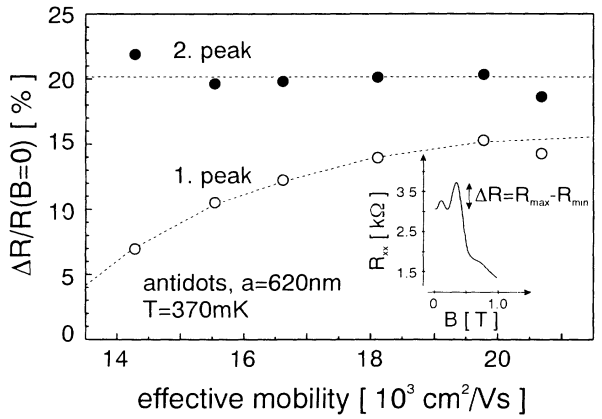

FIG. 3. Ratio of peak height ΔR to longitudinal resistance R at $B=0$ for the two low-field peaks arising from pinned orbits around four (1. peak, hollow symbols) or one (2. peak, filled symbols) antidots as a function of the effective mobility for the sample with period $a=620$ nm. Note that $\Delta R/R(B=0)$ remains roughly constant for the second peak while the first peak gains intensity with increasing mobility. The dashed lines are guides to the eye.

In addition to ρ_{xx}, Fig. 2(b) also displays the Hall resistance R_{Hall} of the specimen with period $a=620$ nm both in the dark and after intensive illumination. While the well-known quantum-Hall plateaus can be seen for magnetic fields greater than $B=2$ T, two additional, nonquantized plateaus are observed at fields slightly higher than those of the peaks in ρ_{xx}, indicated by the two arrows. Around $B=0$ the Hall effect is quenched in the sense that, even through R_{Hall} is not zero at finite fields, its dependence on the magnetic field is by no means linear. The two "last plateaus" and the quenching of the Hall effect are typical transport phenomena in antidot superlattices. Fleischmann, Geisel, and Ketzmerick[12] have shown in theoretical work that chaotic channeling trajectories occur in a periodic two-dimensional potential at small magnetic fields. These preferentially leave the channel they have been following in the direction opposite to the Lorentz force, resulting in a quenched or negative Hall effect. In the same work it is argued that the additional, nonquantized plateaus are associated with cyclotron-type orbits around one or four antidots. It is also noteworthy that softness of the potential to some degree is absolutely necessary to observe these effects.

All the features we have observed are very similar to those known from work on arrays of antidots in $GaAs/Al_xGa_{1-x}As$ samples performed recently. They are yet another manifestation that high-quality 2DEG's are no longer restricted exclusively to III-V semiconductor structures, but may also be found in the Si/Ge system. Commensurability maxima and Hall-effect anomalies, all of which are typical features of electron transport in antidot arrays, can be well understood by assuming a smooth and rather broad lateral potential,[6,12] It has been shown in Ref. 6 that in this kind of periodic potential pinned trajectories will only be possible around one or four antidots and that the larger orbit will be strongly noncircular. The existence of smooth potential walls in the antidot superlattice also explains the well-pronounced, anomalous plateaus in R_{Hall}. The above assumption about the potential indeed appears to be realistic in our case since softness is expected to arise from depletion of the antidot walls. Also, the antidots' diameter d_{GEO} is rather large compared to their period a.

Furthermore, the lateral potential might be inhomogenously broadened resulting from the slightly inhomogenous etch depths caused by the crosshatched surface pattern. One should also keep in mind that the electron mobilities still differ from those in $GaAs/As_xGa_{1-x}As$

heterostructures by almost an order of magnitude. To be able to see commensurability maxima arising from pinned orbits around more than four antidots, as observed by Weiss *et al.*,[2] it is thus necessary to further reduce both the period a and simultaneously the ratio d_{GEO}/a.

In summary, we have studied electron transport in lateral antidot superlattices in Si/SiGe heterostructures. Typical magnetotransport features such as low-field commensurability maxima in ρ_{xx} associated with pinned orbits around one or four antidots, additional Hall plateaus, and quenching of the Hall effect were observed. Our experimental results can be well explained by assuming that the lateral potential generated by laser holography with successive reactive-ion etching is rather smooth and also affected by inhomogenous broadening.

We would like to thank K. Ensslin for valuable discussions. This work was financially supported in part by the Siemens AG (SFE Mikrostrukturierte Bauelemente) and by the Bundesministerium für Forschung und Technologie (Bonn, Germany) under Grant No. NT 24137.

[1]K. Ensslin and P. M. Petroff, Phys. Rev. B **41**, 12 307 (1990).
[2]D. Weiss, M. L. Roukes, A. Menschig, P. Grambow, K. von Klitzing, and G. Weimann, Phys. Rev. Lett. **66**, 2790 (1991).
[3]A. Lorke, J. P. Kotthaus, and K. Ploog, Phys. Rev. B **44**, 3447 (1991).
[4]R. Schuster, K. Ensslin, J. P. Kotthaus, M. Holland, and C. Stanley, Phys. Rev. B **47**, 6843 (1993).
[5]D. Weiss, K. Richter, A. Menschig, R. Bergmann, H. Schweizer, K. von Klitzing, and G. Weimann, Phys. Rev. Lett. **70**, 4118 (1993).
[6]R. Fleischmann, T. Geisel, and R. Ketzmerick, Phys. Rev. Lett. **68**, 1367 (1992).
[7]W. Kang, H. L. Störmer, L. N. Pfeiffer, K. W. Baldwin, and K. W. West, Phys. Rev. Lett. **71**, 3850 (1993).
[8]F. Schäffler, D. Többen, H.-J. Herzog, G. Abstreiter, and B. Holländer, Semicond. Sci. Technol. **7**, 260 (1992).
[9]S. F. Nelson, K. Ismail, T. N. Jackson, J. J. Nocera, J. O. Chu, and B. S. Meyerson, Appl. Phys. Lett. **63**, 794 (1993).
[10]Y. H. Xie, E. A. Fitzgerald, D. Monroe, P. J. Silverman, and G. P. Watson, J. Appl. Phys. **73**, 8364 (1993).
[11]D. Többen, F. Schäffler, A. Zrenner, and G. Abstreiter, Phys. Rev. B **46**, 4344 (1992).
[12]R. Fleischmann, T. Geisel, and R. Ketzmerick, Europhys. Lett. **25**, 219 (1994).